

Proceedings Article

Traveling Wave MPI utilizing a Field-Free Line

C. Greiner^{a,*}, M. A. Rückert^a, T. Kampf^{a,b}, V. C. Behr^a, P. Vogel^a

^aDepartment of Experimental Physics 5 (Biophysics), University of Würzburg, 97074, Würzburg, Germany

^bDepartment of Diagnostic and Interventional Neuroradiology, University Hospital Würzburg, 97080, Würzburg, Germany

*Corresponding author, email: Christoph.Greiner@physik.uni-wuerzburg.de

© 2022 Greiner *et al.*; licensee Infinite Science Publishing GmbH

This is an Open Access article distributed under the terms of the Creative Commons Attribution License (<http://creativecommons.org/licenses/by/4.0>), which permits unrestricted use, distribution, and reproduction in any medium, provided the original work is properly cited.

Abstract

Field-free line (FFL) Magnetic Particle Imaging (MPI) scanners are of high interest for fast and accurate scanning of 3D samples because of the higher signal-to-noise ratio due to the enlarged encoding scheme. Until now, only magnetic field generators have been presented providing an electrical rotation and displacement of an FFL within a 2D slice. Utilizing double-helix coils and the Traveling Wave approach, a full 3D FFL MPI scanner can be introduced, providing fast 3D imaging with less hardware efforts.

I. Introduction

Since the first publication of Magnetic Particle Imaging (MPI) in 2005 by B. Gleich and J. Weizenecker [1], multiple different scanner designs have been presented [2]. The basic idea behind MPI is to measure the non-linear magnetization response of superparamagnetic iron-oxide nanoparticles (SPIONs) to time-varying magnetic fields. For encoding, a strong magnetic field gradient is rapidly moved through the field of view (FOV) inducing MPI signal in the receive coil by the change of the SPION magnetization. Two different encoding schemes have been presented: field-free point (FFP) and field-free line (FFL).

Originally, FFP scanners used either permanent magnets [1, 3] or electromagnets [4, 5, 6] assembled in Maxwell configuration for the generation of a static FFP in the center of the system. Using additional drive-coils in Helmholtz configuration, the FFPs can be steered on specific trajectories covering the entire FOV. For scanning FOVs of the size of a whole rodent, the Traveling Wave MPI scanner has been presented in 2014 using a dynamic linear gradient array (dLGA) generating and moving multiple FFPs dynamically along the scanner [7, 8]. All FFP scanners provide high acquisition speed [9, 10], high sensitivity [11] and good spatial resolution [12].

FFL scanners firstly have been introduced in 2008 [13]. Their more complex setup using permanent or electro magnets allows the generation, movement and rotation of an FFL, which provides the acquisition of projections of the sample with a higher signal-to-noise ratio (SNR) [14, 15, 16, 17, 18]. However, the complex hardware requirements for magnetic field generation only allow for fast 2D signal acquisition. For 3D scanning, additional mechanical parts are required, i.e., a mechanically rotated gantry.

In this abstract, a novel MPI scanner design is presented, which provides dynamic 3D projection imaging using an FFL entirely generated by electro magnets.

II. Material and methods

The basic idea behind this novel approach is the dLGA concept used in TWMPI scanners [7, 8]. In a dLGA-4 system four solenoids, fed with the same sinusoidal current with frequency f_1 and a phase shift between adjacent coils of 90° , are used to generate traveling FFPs along the symmetry axis. By replacing the four solenoids in the dLGA-4 by a double-helix dipole coil design (DHD or cross-coil – CC) [19], a field-free line traveling along the

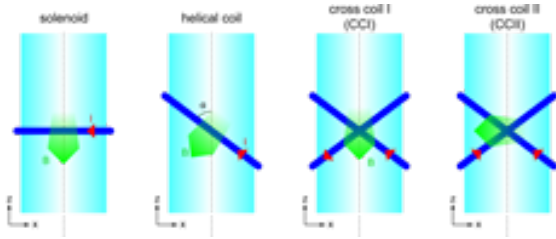


Figure 1: Evolution from single solenoid to cross-coil concept.

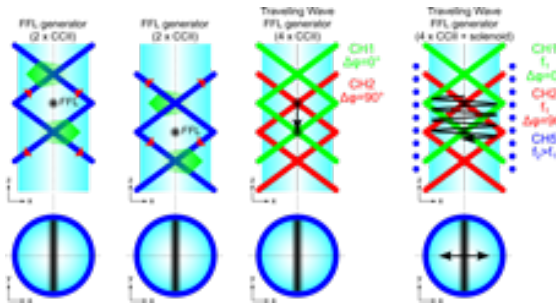


Figure 2: Concept of the Traveling Wave FFL generator. The dark regions at the bottom indicate the FFL.

symmetry axis can be generated.

In Fig. 1 the concept is shown: a single solenoid is tilted and complemented by a second one to form a cross-coil. Depending on the direction of current (CCI and CCII), the magnetic field direction can be adjusted in x- and z-direction.

Assembling two cross-coils with configuration II (CCII) along the z-axis, where the magnetic field direction is inverted (compare Maxwell configuration of two solenoids), a static field-free line is generated in their center (see Fig. 2). Adding a second pair of CCII coils and feeding both with a sinusoidal current and a phase shift of 90°, the FFL travels along the symmetry axis (Traveling Wave approach [7]).

A solenoid assembled around the entire system allows to translate the FFL in the x-y-plane regardless of its orientation. With this generator, a full projection through the FOV can be provided. For FFL rotation around the z-axis an additional Traveling Wave FFL Generator (4xCCII coils) is assembled in perpendicular orientation (90° rotated around z-axis). At the end, five independent chan-

Table 1: Overview about the channels and frequencies driving a full 3D FFL scanner.

Channel	
CH 1	$A \cdot \sin(2\pi f_1) \cdot \sin(2\pi f_2)$
CH 2	$A \cdot \sin(2\pi f_1 + \pi/2) \cdot \sin(2\pi f_2)$
CH 3	$A \cdot \sin(2\pi f_1) \cdot \sin(2\pi f_2 + \pi/2)$
CH 4	$A \cdot \sin(2\pi f_1 + \pi/2) \cdot \sin(2\pi f_2 + \pi/2)$
CH 5	$B \cdot \sin(2\pi f_3)$

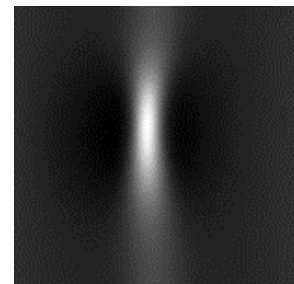
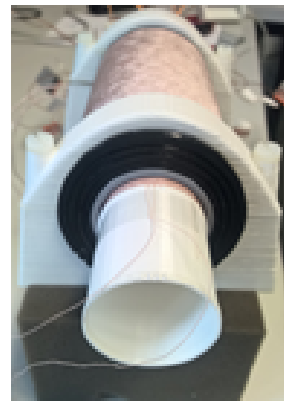
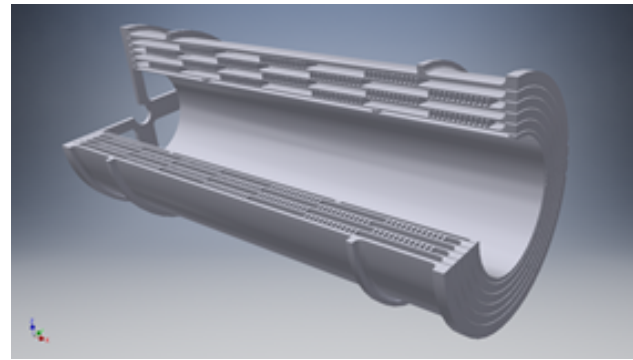


Figure 3: Top: CAD rendering of the 3D printable coil holders. Bottom left: photo of the first prototype of the TWMPI FFL scanner. Bottom right: first measurement of a point-like sample.

nels (CH1..CH4 feeding the cross-coils and CH5 feeding the solenoid) running at three frequencies ($f_1 \dots f_3$) are required to move the FFL within the 3D volume (see Table 1).

III. Results and discussion

In initial simulation studies with a home-built simulation framework [20], the geometry and field performance of the TWMPI FFL scanner has been determined for a FOV with length 70 mm and 30 mm diameter and gradient strength of about 1.5 T/m. In Fig. 3 top, a CAD rendering of the 3D printable coil holders can be seen providing multiple layers for the cross-coils and the solenoid.

In Fig. 3 bottom left, a photo of the first TWMPI FFL scanner is shown. For an easy fabrication and space-saving assembling of the cross-coils, a special winding technique is used providing compact dimensions of the entire scanner of 158 mm in length and 70 mm in diameter.

In Fig. 3 bottom right, the first result of a 2D scan of a point-like sample is demonstrated (frequencies: $f_1=220.4$ Hz, $f_2=0.0$ Hz, $f_3=9329.9$ Hz).

IV. Conclusions

The TWMPI FFL scanner design uses a novel approach for the dynamic generation, movement and rotation of a field-free line. This allows scanning full 3D samples with short acquisition times and the advantages of a higher SNR. Since the hardware requirements are small, compact scanners can be built, which can revolutionize pre-clinical usage of MPI.

Acknowledgments

Research funding: The work was funded by the German Research Council (DFG) (grant numbers: VO-2288/1-1, VO-2288/2-1, BE-5293/1-2).

Author's statement

Conflict of interest: Authors state no conflict of interest.

References

- [1] B. Gleich & J. Weizenecker, Tomographic Imaging using the nonlinear response of magnetic particles, *Nature*, 435, 1214-7, 2005.
- [2] T. Knopp et al., Magnetic Particle Imaging: From Proof of Principle to Preclinical Applications, *Phys Med Biol*, 62(14), R124, 2017.
- [3] H. Bagheri et al., A mechanically driven magnetic particle imaging scanner, *Appl Phys Lett*, 113:183703, 2018.
- [4] J.J. Konkle et al., A Convex Formulation for Magnetic Particle Imaging X-Space Reconstruction, *PloS One*, 10(10):e0140137, 2015.
- [5] P.W. Goodwill & S.M. Conolly, Multidimensional x-space magnetic particle imaging, *IEEE TMI*, 30(9), 1581-90, 2011.
- [6] J. Franke et al., System Characterization of a Highly Integrated Pre-clinical Hybrid MPI-MRI Scanner, *IEEE TMI*, 35(9), 1993-2004, 2016.
- [7] P. Vogel et al., Traveling Wave Magnetic Particle Imaging, *IEEE TMI*, 33(2), 400-7, 2014.
- [8] P. Vogel & P. Klauer et al., Dynamic Linear Gradient Array for Traveling Wave Magnetic Particle Imaging, *IEEE Trans Magn*, 54(2):5300109, 2018.
- [9] P. Vogel et al., Superspeed Traveling Wave Magnetic Particle Imaging, *IEEE Trans Magn*, 51(2):6501603, 2015.
- [10] J. Weizenecker et al., Three-dimensional real-time in vivo magnetic particle imaging, *Phys Med Biol*, 54(5):L1-10 2009.
- [11] M. Graeser et al., Towards Picogram Detection of Superparamagnetic Iron-Oxide Particles Using a Gradiometric Receive Coil, *Sci Rep*, 7:6872, 2017.
- [12] P. Vogel et al., Micro Traveling Wave Magnetic Particle Imaging – sub-millimeter resolution with optimized tracer LS-008, *IEEE Trans Magn*, 55(10):5300207, 2019.
- [13] J. Weizenecker et al., Magnetic Particle Imaging using a field free line, *J Phys D*, 41(10):105009, 2008.
- [14] P.W. Goodwill et al., Projection X-Space Magnetic Particle Imaging, *IEEE TMI*, 31(5), 1076-85, 2012.
- [15] K. Bente et al., Electronic field free line rotation and relaxation deconvolution in magnetic particle imaging, *IEEE TMI*, 34(2), 644-51, 2015.
- [16] P. Vogel et al., Magnetic Particle Imaging meets Computed Tomography: first simultaneous imaging, *Sci Rep*, 9:12627, 2019.
- [17] P. Vogel et al., MPI Cube – fully 3D field free line scanner, *Proc. on IWMPPI (Lübeck)*, p26, 2016.
- [18] K. Lu et al., Multi-channel Acquisition for Isotropic Resolution in Magnetic Particle Imaging, *IEEE TMI*, 37(9), 1989-98, 2017.
- [19] C.L. Goodzeit et al., The double-helix dipole - a novel approach to accelerator magnet design, *IEEE Trans Appl Supercond*, 13(2), 1365-8, 2003.
- [20] P. Vogel et al., 3D-GUI Simulation Environment for Magnetic Particle Imaging, *Proc. on IWMPPI (Lübeck)*, 95, 2016.